JOURNAL OF MATERIALS SCIENCE 31 (1996) 2667–2676

X-ray photoelectron spectroscopy and Auger electron spectroscopy of the influence of cations and anions of organometallic adhesion promoters on the interface between steel cord and rubber skim compounds

A. K. CHANDRA, R. MUKHOPADHYAY
R and D Centre, J.K. Industries Ltd, Kankroli 313 342, Rajasthan, India
J. KONAR, T.B. GHOSH, A.K. BHOWMICK*
Rubber-Technology Centre, Indian Institute of Technology, Kharagpur 721 302, India

The influence of cations and anions of the adhesion promoters on the interface between brass-coated steel cord and natural rubber skim compounds has been studied by employing Auger electron spectroscopy and X-ray photoelectron spectroscopy at three different etching times. Cobalt stearate, cobalt boroacylate and nickel boroacylate have been used as organometallic adhesion promoters. The atomic concentrations of sulfur and carbon decreased, while those of copper and zinc increased significantly with etching times. Cobalt/nickel was only found at higher etching times. Cobalt boroacylate increased the atomic concentration of copper, zinc and sulfur with the formation of Cu_xS and ZnS on the top two layers more than the nickel boroacylate. The sulfidation reaction was, however, only partial in the presence of cobalt stearate, and ZnO was observed in the top layer. The atomic concentrations of copper and zinc were also much lower than those of the system containing cobalt boroacylate. A model, based on the results, is proposed to show the difference in activity of the cations and anions.

1. Introduction

In the performance of steel-reinforced tyres, the adhesion between steel cord and rubber plays a vital role. However, the steel does not adhere to the rubber to the degree needed. Hence, two main groups of adhesion promoters – a resin former (SRH-silica, resorcinol and hexamethyl melamine system) and an organometallic promoter, either individually or jointly, are used in the rubber compound in order to obtain adequate adhesion and durability necessary for the life-span and performance requirements of the product [1–7]. Moreover, incorporation of cobalt promoter greatly enhances the adhesion energy and influences the compound properties and cross-link density [8, 9]. Several authors [10–16] studied the influence of these systems on the static and dynamic adhesion between rubber and brass-coated steel cord.

However, these brass-coated steel cords are prone to severe electrochemical corrosion in saline and humid environments [17, 18]. As a result, pitting corrosion of the steel cord core and dezincification of the brass coating, often observed in tyres subjected to road tests, weaken the reinforcing effect of the cord and lead to the loss of cord–rubber adhesion, thus, reducing the service life of a steel cord-reinforced tyre [19]. To reduce the effect of deleterious corrosion processes encountered by brass coating under different hostile environments, it is essential to understand the mechanism of bond formation, adhesion degradation and characteristics of the actual rubber–steel cord interface. Characterization of rubber–steel cord interfaces after tyre failures has been studied by Seitz and Schmidt [20, 21]. They discussed various possible types of corrosion in radial tyres. Coppens *et al.* [22] studied the brass–rubber interface without separating the rubber from the metal, mechanically or chemically. Their method involved depth profiling by Auger electron spectroscopy (AES) and X-ray photoelectron spectroscopy (XPS) through a very thin brass film bonded to a rubber substrate. Van Ooij [18, 19, 23] and Madura [24] investigated rubber to metal bond failures by sensitive surface-analytical techniques. Scanning electron microscopy (SEM) coupled with energy dispersive X-ray spectroscopy (EDXS), secondary ion mass spectrometry (SIMS) and Argon-ion depth profiling coupled with XPS or AES, were used in these studies to determine the composition of the

*Author to whom all correspondence should be addressed.

0022–2461

metal surfaces. Bhowmick *et al.* [25–27] used XPS to understand surface modification of polymers, tack, diffusion, milling and ageing of rubbers.

The literature survey reveals that there is no systematic study of the influence of organometallic adhesion promoters on the interface between steel cord and rubber compounds. Moreover, those studies made so far on the rubber–brass interface were based on bulk brass sheet (not on brass-coated steel cord) using a model compound of squalene. Such studies (i.e. with steel cord and actual rubber formulation) may have been carried out in several laboratories associated with cord suppliers and tyre manufacturers, but very little observation has been published so far.

The objective of this study was to describe the influence of cations and anions of the adhesion promoters on the interface between brass-coated steel cord and rubber compound (typical steel cord–skim formulation used in the tyre industry).

2. Experimental procedure

2.1. Materials

The details of the materials used for the present study are shown in Table I. Other chemicals not included in the table were received from the standard Indian suppliers.

2.2. Mixing and moulding of tyre cord adhesion test (TCAT) specimens

A complete list of the mixes used in the present investigation, together with their physical properties, is given in Table II.

Mixing was carried out in three stages using a Laboratory Banbury of capacity 1.2 kg (batch weight; Stewart Bolling USA) having a two-wing rotor (Model 00). All ingredients, except organometallic adhesion promoters, methylene donor and vulcanizing agents, were mixed in the masterbatch stage. These batches were remilled in the Banbury in the next stage. In the final stage, the remaining ingredients were added. After dumping, the batches were sheeted out using a Laboratory two-roll mixing mill and covered in polyethylene.

These formulations were utilized for preparing the tyre cord adhesion test (TCAT) specimens having dimensions 10.0 mm × 12.0 mm × 50.0 mm (Fig. 1) with 20.0 mm cord embedment length. TCAT samples were cured for 2 h at 141 °C by compression moulding techniques. Details of mixing and moulding of TCAT specimens were described elsewhere [8, 9].

2.3. Testing

2.3.1. Cure characteristics, Mooney viscosity and physical properties

Cure characteristics of the specimens were studied using a rheometer (Monsanto MDR-2000) at 141 °C

TABLE I (a) Materials used for the study

Materials	Grade	Suppliers
Natural rubber	RMA-4	Kerala, India
Methylene donor	Cohedur-4	Bayer AG, Germany
Homogeneous solidified melt of resorcinol and stearic acid in the ratio of 2:1 (methylene acceptor; resorcinol component)	Cohedur-RS	Bayer AG, Germany
N-phenyl-*N'* (1,3-dimethyl butyl)-*p*-phenylene diamine	Vulkanox-4020 (Antioxidant-6PPD)	Bayer AG, Germany
N, *N*-dicyclohexyl-2-benzothiazole sulfenamide	Vulkacit-DZ (Accelerator DCBS)	Bayer AG, Germany
Hydrated silicon dioxide (pptd. silica)	Ultrasil-VN3	Degussa AG, Germany
Octyl phenol formaldehyde resin		CECA, SA, France
Insoluble sulfur (20% highly non-staining naphthenic oil treated)	Crystex OT-20	Kali Chemical, Germany

(b) *Organometallic Adhesion Promoters*

	Metal content (%)	Grade	Suppliers
Cobalt stearate	9.5	CS-95	Manchem Ltd, UK
Cobalt boroacylate	23.0	680C	Manchem Ltd, UK
Nickel boroacylate	6.0	Manocat NBA	Manchem Ltd, UK

(c) Steel cord

Style 7 mm × 4 mm × 0.2 mm[a]	Tokyo Rope, Japan
Lay length, direction (mm) 10S/14Z	
Plating composition 67.5 ± 1.0% Cu; 32.5 ± 1.0% Zn	
Plating density 6.0 ± 0.5 g kg^{-1}	
Nominal diameter 1.5 mm	

[a]This cord is basically a commercial truck tyre cord. The convention used in wire and tyre industries is followed for writing the construction.

TABLE II Formulations and characterization of the mixes

Ingredients (parts of metal ion per hundred g rubber	Mix			
	A	B	C	D
Cobalt stearate	–	0.25	–	–
Cobalt boroacylate	–	–	0.25	–
Nickel boroacylate	–	–	–	0.25
Mooney viscosity (ML_{1+4} at 100 °C)	85.3	69.8	89.3	77.2
Scorch time, t_2, (min)	5.5	5.0	5.2	6.3
Optimum cure time, t_{90} (min)	38.6	29.2	28.7	35.0
Reversion (t_{98}) after crossing maxima (min)	No reversion up to 90 min	71.0	75.0	77.0
V_r	0.286	0.310	0.299	0.302
IRHD	80	87	85	84
100% modulus (MPa)	6.75	8.0	7.85	8.30
200% modulus (MPa)	14.45	16.15	15.25	16.7
Tensile strength (MPa)	20.8	18.5	16.7	18.5
Elongation at break (%)	290	225	220	235
Energy to break (kJ m^{-2})	22.4	16.1	14.1	16.9
Energy of Adhesion (kJ m^{-2})	35.5	36.5	43.0	40.0

All mixes contain (p.h.r.), NR 100; peptiser (activated PCTP) 0.1; carbon black (HAF, N330) 60; aromatic oil 6; Cohedur RS 3.5; pptd. silica 10; ZnO 10; stearic acid 0.25; 6PPD 2.0; PF resin 2.5; insoluble sulfur 6.0; DCBS 1.0; Cohedur-A 2.25.

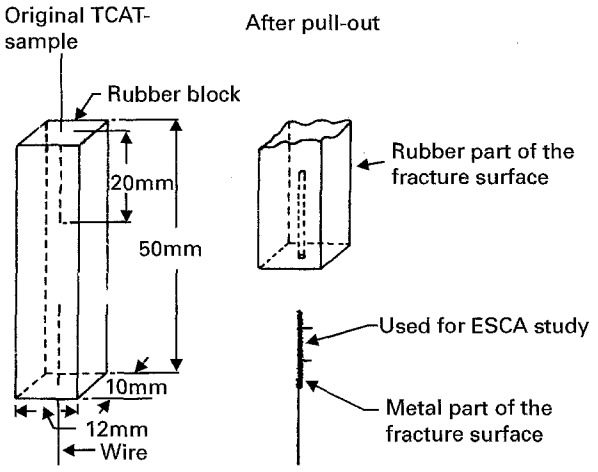

Figure 1 TCAT samples for XPS measurements.

temperature. A Monsanto Mooney viscometer (MV-2000) was used to determine Mooney viscosity as per ASTM D1646.

Physical properties (stress–strain) reported in Table II, were determined as per the ASTM method (ASTM D412) using a Zwick Universal Testing system (model 1445) at a crosshead speed of 500 mm min^{-1}. Hardness of the specimens was determined using an IRHD-Hardness Tester (H.W. Wallace and Co. Ltd, UK) as per ASTM D1415.

2.3.2. TCAT test

For XPS measurement, the samples were prepared as follows: the two opposite axial free cord ends of a TCAT sample (Fig. 1) were clamped in a Zwick Universal Testing machine and pulled at a rate of 50 mm min^{-1} at 25 ± 2 °C. To study the nature of the interface by XPS, the failed metal surface after the pull-out test was dipped in xylene for 12 h at room temperature (25 ± 2 °C). Then, it was rubbed gently with a tissue paper to remove the swollen rubber vulcanisate from the steel cord. The number of times a wire was rubbed was kept constant for all wires to ensure that each sample received the same degree of light mechanical abrasion [28].

2.3.3. XPS study

XPS measurements were performed in a VG Scientific ESCA LAB MK II spectrometer, operating at a pressure of 1×10^{-8} torr (1 torr = 133.322 Pa), with AlK_α

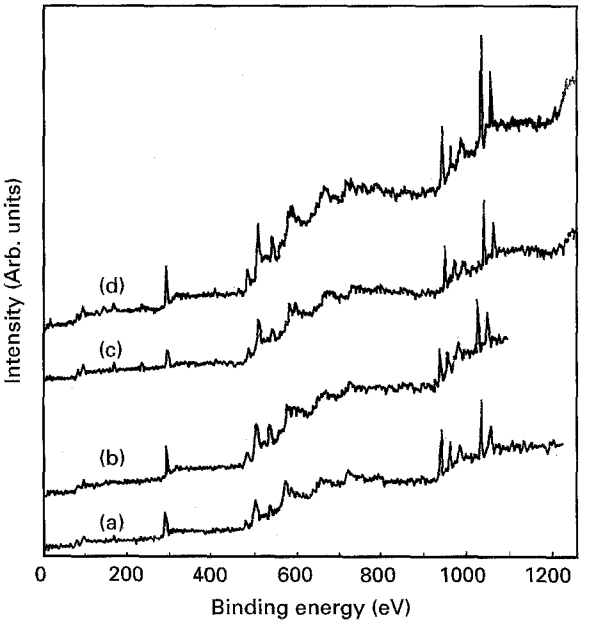

Figure 2 XPS survey scan for the system containing (a) no adhesion promoter, (b) system containing cobalt stearate, (c) system containing cobalt boroacylate, and (d) system containing nickel boroacylate.

radiation (1486.6 eV). Each specimen was analysed by a combination of 1250 eV survey and 25 eV high-resolution scans for all the peaks [29]. High-resolution spectra were recorded at 40 eV pass energy for which instrumental resolution was ± 0.8 eV. All the samples were etched for 2, 7 and 15 min at 7 kV with 50 μA target current using argon gas at 25 °C. To obtain the stoichiometry, the published values of the sensitivity factors [30] were used. Under these conditions, the predicted stoichiometry is expected to be within 10 atomic % [31].

2.3.4. Determination of the chemical states

Chemical states of the elements were determined from the relative chemical shift between the photoelectron and the Auger electron spectrum. The Auger parameter, α, was defined as α = KE (Auger) + BE (photoelectron), where KE (Auger) is the Auger line position expressed in kinetic energy and BE (photoelectron) is the photoelectron line position measured in binding energy scale. The measured positions of the photoelectron and Auger electron lines were used to determine α for the various compositions.

3. Results and discussion

Survey scan spectra of various samples are shown in Fig. 2. The binding energy values of 163, 285, 532, 784, 854, 932 and 1022 eV correspond to sulfur, carbon, oxygen, cobalt, nickel, copper and zinc, respectively. Auger lines of copper and zinc appear at 498 and 570 eV, respectively. The atomic concentration of various elements changes with the etching time as well as the nature of the cation or the anion and the ageing conditions. In order to quantify this, the regions around these elements have been expanded and these spectra are shown in Figs 3–6. The expanded spectra are also helpful in predicting the chemical states of the various elements. Table III records the atomic concentrations of sulfur, carbon, oxygen, cobalt, nickel, copper and zinc at various etching times. The Cu/Zn ratio was also calculated.

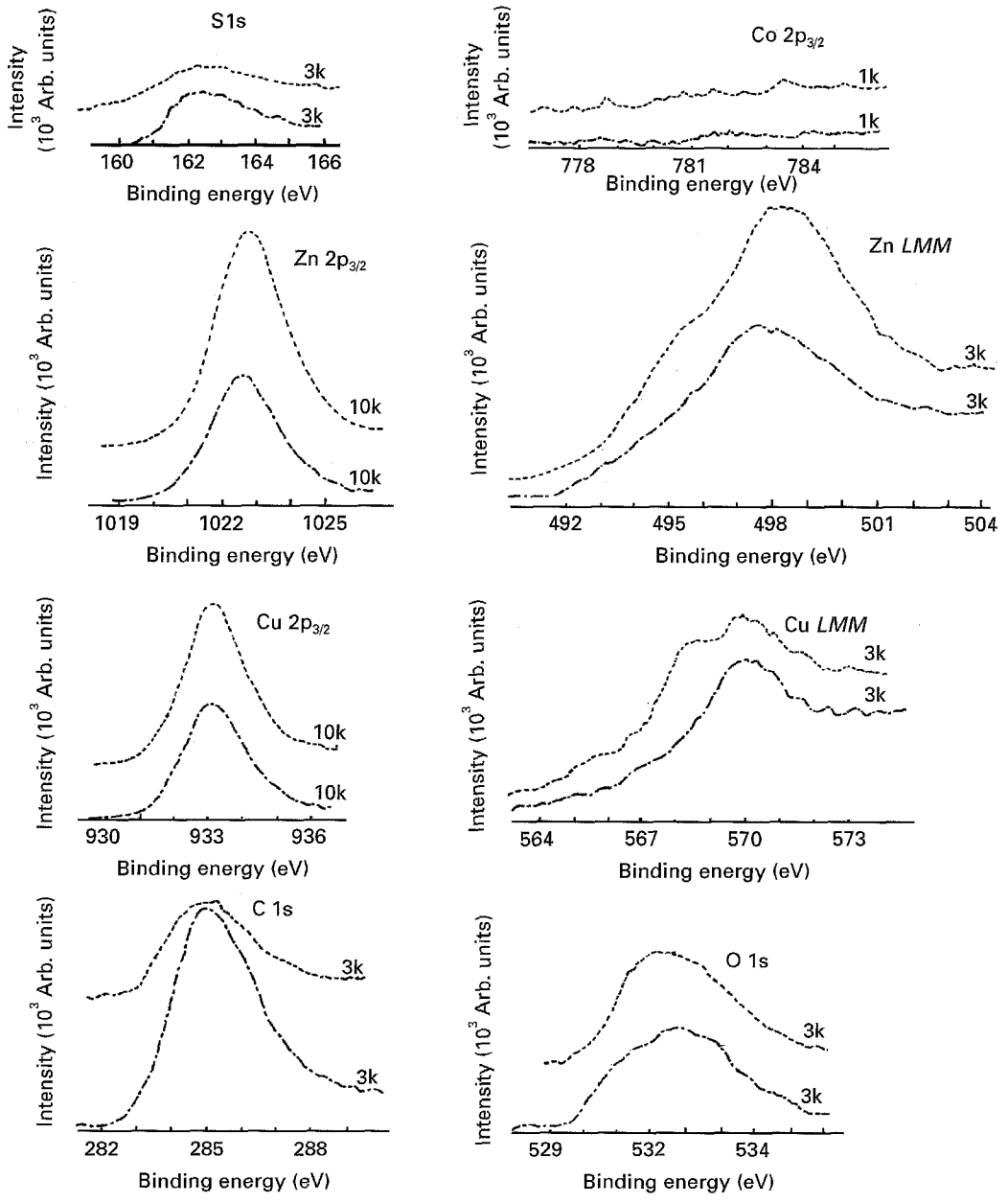

Figure 3 Expanded XPS and AES peaks for sample A (control compound), (———) 2 min etching and (– – –) 7 min etching.

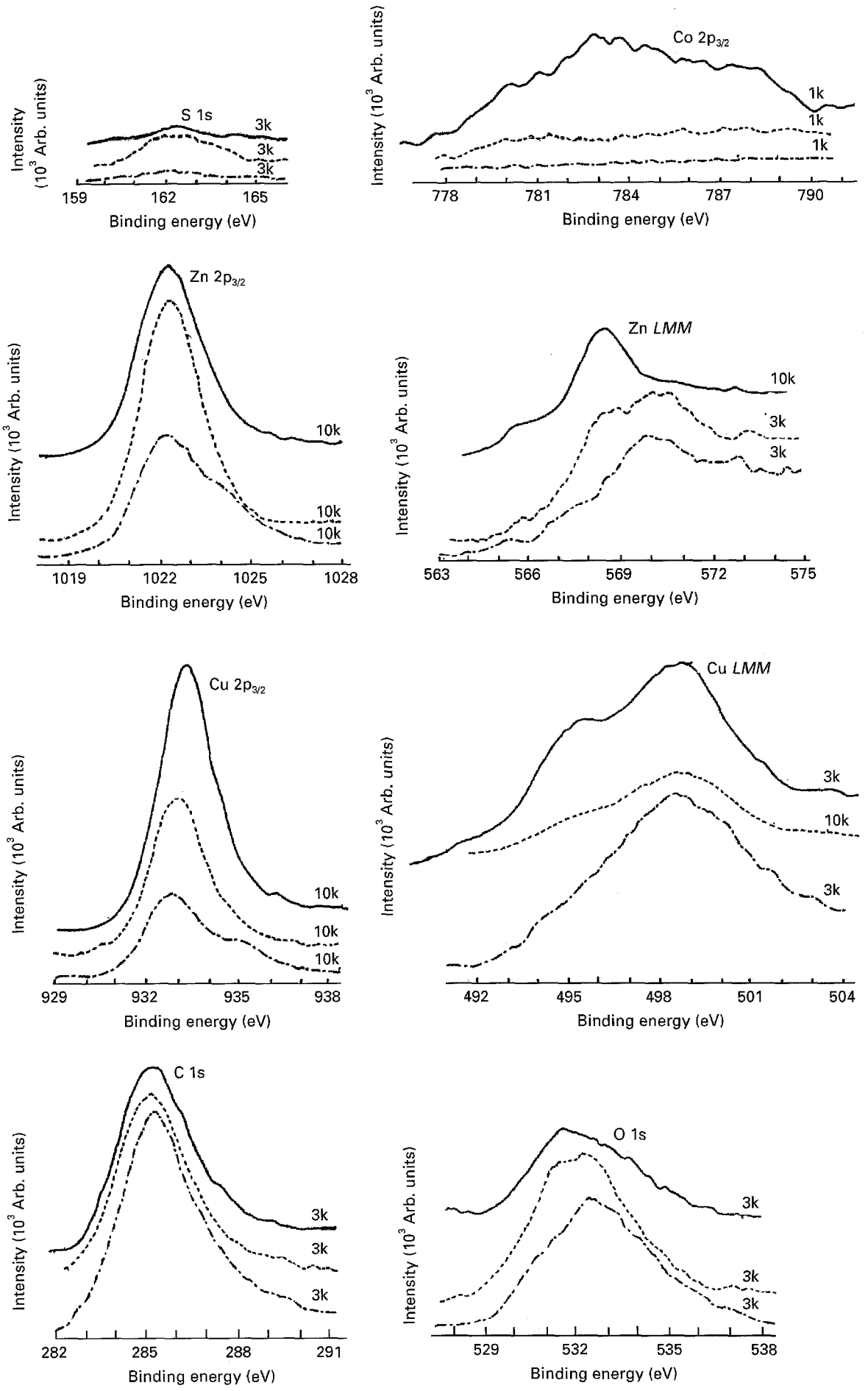

Figure 4 Expanded XPS and AES peaks for sample B (system containing cobalt stearate), (———) 2 min etching, (– – –) 7 min etching, and (——) 15 min etching.

It was observed that the atomic concentration of sulfur and carbon decreases with etching time. Oxygen increased marginally in the initial stage before a final decrease at 15 min etching. The percentage of both copper and zinc increased significantly. Cobalt/nickel was only found at higher etching times. The ratio of Cu/Zn increased for all the samples, except A. In bare brass-coated steel cord, etched for 10 min, the ratio of Cu/Zn was found to be 1.0 ea. The latter observation is well supported by earlier work [18].

At a particular etching time, when samples A (control) and C (the sample containing cobalt boroacylate) are compared, the sulfur concentration was found to be higher for C and the percentage of oxygen remained the same.

At lower etching time (2 min), the atomic concentrations of copper and zinc increased with the addition of cobalt boroacylate in the system. The data in Table III reveal a marked difference when cobalt boroacylate is replaced by an equal amount of nickel boroacylate.

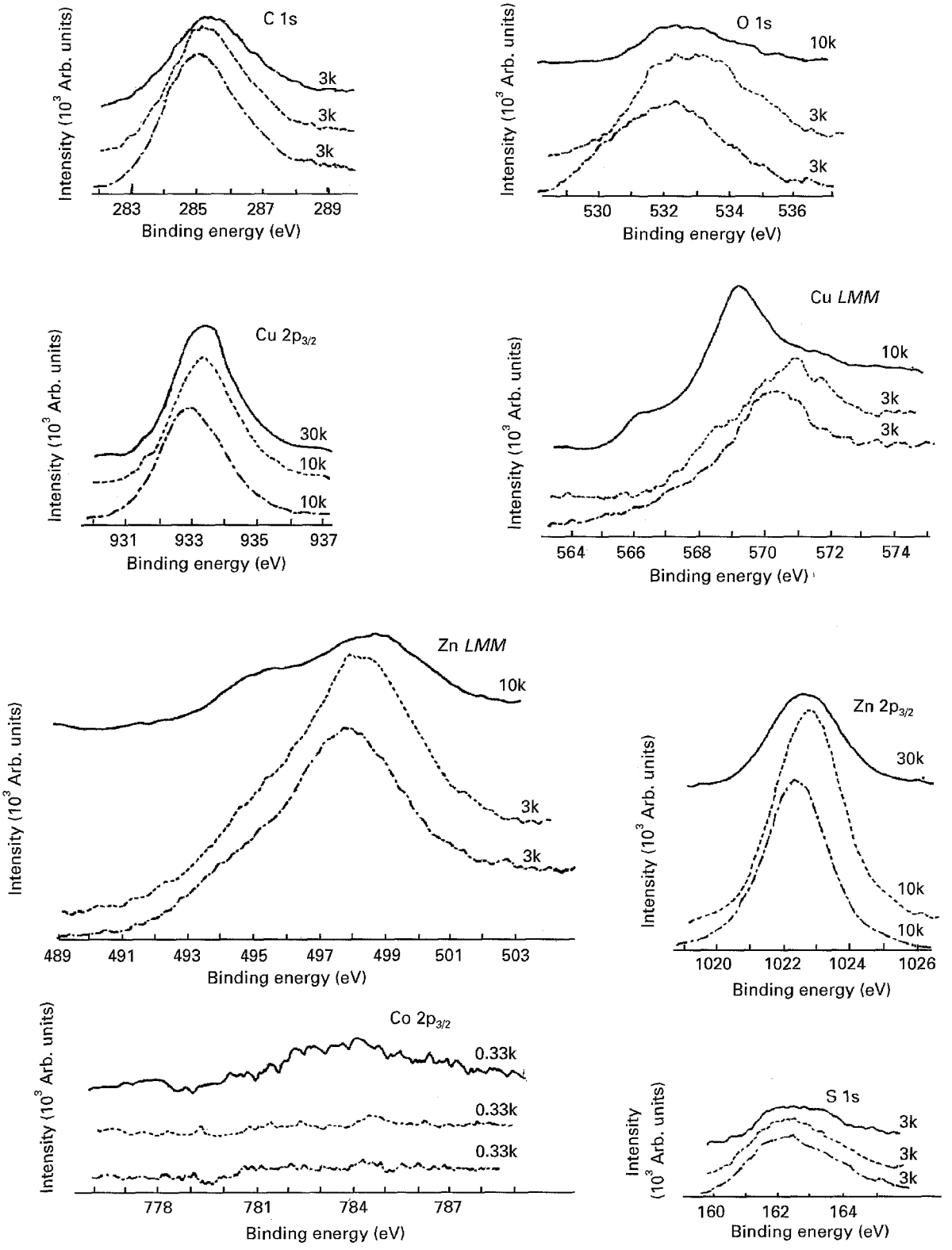

Figure 5 Expanded XPS and AES peaks for sample C (system containing cobalt boroacylate), (———) 2 min etching, (– – –) 7 min etching, and (——) 15 min etching.

For example, at 2 and 7 min etching times, the sulfur concentration decreased, while the amount of oxygen and carbon did not change appreciably. The percentage of copper showed a marked reduction in the case of nickel boroacylate system. Although there was no change in the zinc concentration at 2 and 7 min etching times, there was a decreasing trend at 15 min etching and the ratio of copper and zinc was lowered in the nickel system. The change of anion (mixes B and C) also gave very interesting results. The sample prepared with cobalt stearate system registered a decrease in sulfur and a marginal increase in carbon and oxygen. The atomic concentrations of copper and zinc for the stearate system were lower than those of the boroacylate system. Also, the cobalt concentration at 15 min etching time was much greater for sample B. The ratio of copper to zinc at higher concentration, as shown in Table III, is comparable.

3.1. Chemical states of the elements

The changes of chemical states determined from Auger electron spectroscopy and XPS with etching time are presented in Table IV. From the table, it can be inferred that the surface of sample C up to 7 min etching consists of mainly Cu_xS and ZnS, while beyond 15 min etching the surface shows the presence of Cu/CuO, ZnO/ZnS layer and Co^{3+}. The surface of

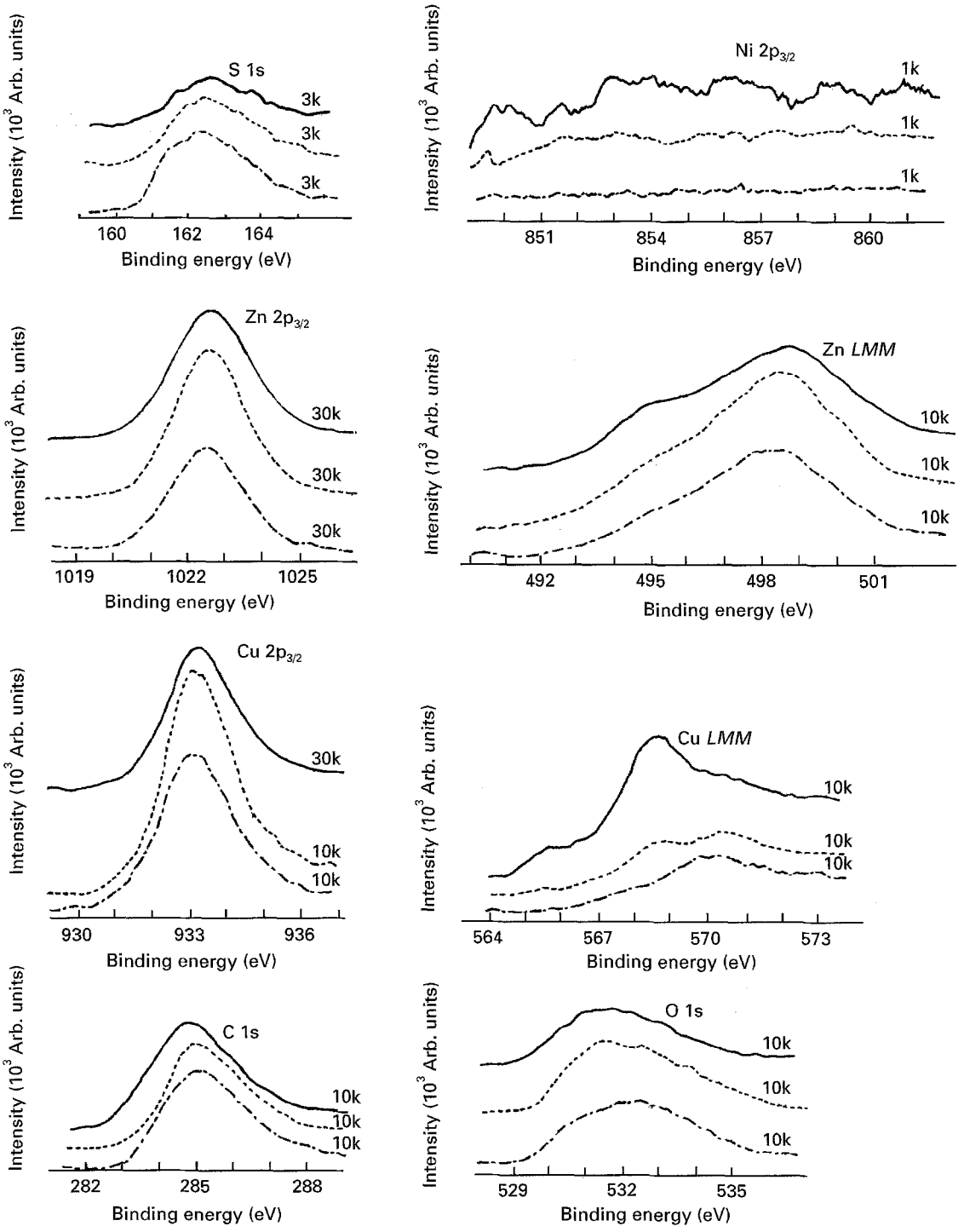

Figure 6 Expanded XPS and AES peaks for sample D (system containing nickel boroacylate), (———) 2 min etching, (– – –) 7 min, etching, and (——) 15 min etching.

TABLE III Atomic concentration (%) of various elements

Sample	Etching time (min)	S	C	O	Cu	Zn	Co/Ni	Cu/Zn ratio
A	2	5.7	68.9	14.5	5.4	5.3	–	1.018
	7	5.3	43.8	24.6	11.5	14.7	–	0.782
B	2	–	70.2	19.6	4.5	5.7	–	0.789
	7	4.0	55.0	22.5	7.8	10.3	–	0.757
	15	0.9	58.8	14.6	13.5	9.6	2.4	1.406
C	2	11.2	53.8	17.3	7.1	10.5	–	0.676
	7	10.5	47.2	20.6	9.0	12.6	–	0.714
	15	3.7	34.6	18.7	24.8	17.7	0.4	1.401
D	2	6.4	61.5	17.7	5.2	9.1	–	0.571
	7	5.2	53.6	21.4	6.9	12.7	–	0.543
	15	3.9	50.2	17.9	13.6	13.9	0.4	0.978

TABLE IV Chemical states of copper and zinc in various samples

Sample	Etching time (min)	$Cu2p_{3/2}$	Cu LMM	α_{Cu}	Remarks	$Zn2p_{3/2}$	Zn LMM	α_{Zn}	Remarks
A	2	933.1	570.2	1849.5	Cu_xS	1022.6	498.0	2011.2	ZnS
	7	933.0	570.0	1849.6	Cu_xS	1022.4	498.5	2010.5	ZnO/ZnS
B	2	932.8	569.8	1849.6	Cu_xS	1022.3	498.4	2010.5	ZnO/ZnS
	7	933.0	570.1	1849.5	Cu_xS	1022.4	498.6	2010.4	ZnO/ZnS
	15	932.9	568.4	1851.1	Cu/CuO	1022.3	498.5	2010.4	ZnO/ZnS
C	2	932.9	570.2	1849.3	Cu_xS	1022.2	497.5	2011.3	ZnS
	7	933.5	570.9	1849.2	Cu_xS	1022.7	497.7	2011.6	ZnS
	15	933.1	568.4	1851.3	Cu/CuO	1022.3	498.5	2010.4	ZnO/ZnS
D	2	933.1	570.4	1849.3	Cu_xS	1022.4	497.9	2011.1	ZnS
	7	933.0	570.5	1849.1	Cu_xS	1022.4	498.5	2010.5	ZnO/ZnS
	15	933.2	568.5	1851.3	Cu/CuO	1022.4	498.4	2010.6	ZnO/ZnS

sample A, on the other hand, indicates the presence of ZnO at 7 min etching. In the presence of nickel boroacylate, i.e. sample D, a ZnO/ZnS layer is detected earlier, i.e. at 7 min etching time, and Ni^{3+} is observed in place of Co^{3+} at 15 min etching time. Cu_xS is formed at the upper layer. With the changes in the nature of the anion, i.e. with cobalt stearate, sample B, the chemical states of copper remain the same, but that of zinc is determined to be ZnO/ZnS even at 2 min etching time. The XPS and Auger peak shapes shown in Figs 3–6 corroborate the formation of metallic oxides or sulfides. On the basis of the above observations, the following models are proposed for the brass–rubber interface to explain the data (Fig. 7).

During the drawing process (the process used to make the tyre cord), zinc diffuses to the surface, oxidizes and forms a ZnO layer. This lattice will vary in ZnO amount and homogeneity, depending on the drawing process and conditions used. Copper inclusions are present in the ZnO layer and partially oxidize to Cu_2O. During curing, when brass is exposed to active sulfur, the ZnO surface slowly reacts to form initially some ZnS; but this is rapidly overgrown by Cu_xS. The copper sulfide film may contain ZnS inclusions. Cu_2O, if initially present on top of the ZnO layer, is also converted rapidly to Cu_xS (where x ranges from 1.8–1.97 [18]). This is known as sulfidation.

The amount of Cu_xS formed depends largely on the amount of copper inclusions in the original layer of ZnO. ZnO retards sulfidation, but Cu_2O which is grown on the brass by controlled oxidation, accelerates sulfide growth [7, 12]. Sulfidation ceases when the inclusions are depleted. Owing to the Cu_xS-film formation on the cord during cure, natural rubber-based formulations form a strong bond with the brass-coated steel cord. This bond does not mean development of covalent or Van der Waal's bonds, since natural rubber (NR) does not bond directly to most metals owing to a lack of sufficient surface polarity. The bonds involve a very tight interlocking of the cross-linked polymer matrix and the Cu_xS film. This is further supported by the fact that the reduction in pressure during rubber–brass bonding leads to the loss of adhesion at the Cu_xS–NR interface [7, 18]. There is a minimum critical thickness of Cu_xS for maximum adhesion as well as a maximum thickness above which adhesion begins to drop.

The nature of the brass–rubber interface does not differ much with the addition of cobalt boroacylate. Here, the first two layers (2 and 7 min etching times) consist of Cu_xS and ZnS, whereas the third layer (15 min etching time) has Cu/CuO and ZnO/ZnS. In this layer, cobalt has also been found. This is due to the fact that cobalt has effects relating the Cu_xS layer formation during vulcanization. Cobalt complex dissociates to form Co^{2+} ions at the interface during cure. The ease with which this happens, depends on the type of the complex and relates directly to the adhesion promoter efficiency. The Co^{2+} ions are incorporated into the ZnO layer as Co^{3+} ions [7] at

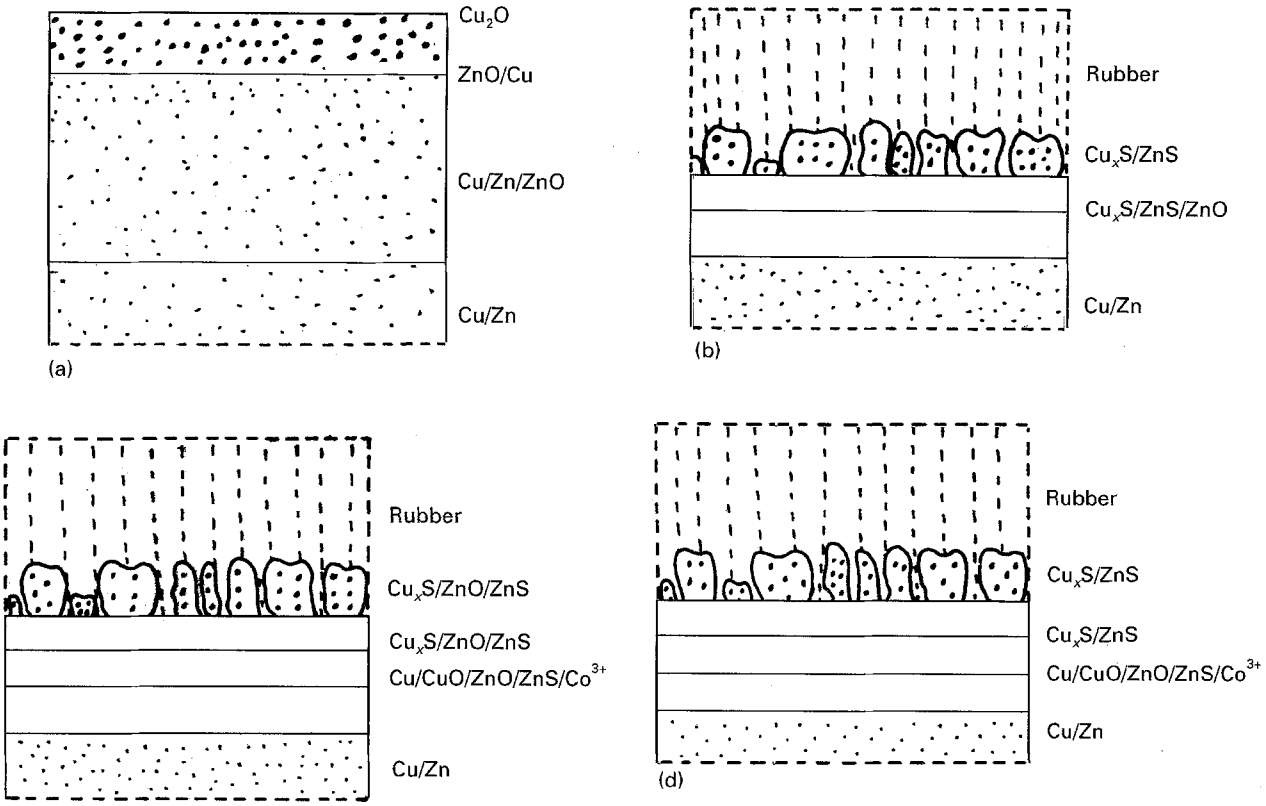

Figure 7 Schematic representation of (a) bare steel, and of the rubber–brass interfacial layer of (b) sample A, (c) sample B, (d) sample C, (e) sample D.

moderate temperatures, before the Cu_xS film has been built up.

During our XPS studies, we noticed that the proportion of copper increases with respect to zinc as we go deeper down from the surface in the presence of cobalt promoter. This clearly indicates that cobalt salts act to inhibit or retard the formation of ZnS at the cord interface and rapid formation of Cu_xS is, therefore, stimulated. Cobalt is presumably present as Co^{3+} in a ZnO lattice and reduces electrical conductivity and the diffusion rate of Zn^{2+} ions through the semiconducting film, i.e. the migration of these ions to the surface may be retarded. Consequently, once the cobalt salt is used, the initial formation of ZnS at the cord surface is suppressed and the rapid formation of Cu_xS is stimulated. This observation is in good agreement with the observations found by earlier workers [18]. Cobalt may also act to increase the surface area of the copper inclusions. All these points are in favour of better bonding which normally takes place in the presence of cobalt promoters [8].

When cobalt boroacylate is replaced by nickel boroacylate, the picture remains almost the same. Even Ni^{3+}, like Co^{3+}, is found in the third layer of Cu/CuO and ZnO/ZnS. Basically, nickel and cobalt, both being members of the transition metal group, behave in the same fashion. However, the presence of nickel discourages the sulfidation reaction. ZnS formation is not speeded up as effectively by nickel as by cobalt, leading to a thicker ZnO layer. This ZnO layer is of paramount importance in the sense that it determines the interfacial reaction, as well as modifying its defect structures. ZnO, being a weak boundary layer, leads to poor adhesion when the thickness is large [18]. In addition to this, Co^{3+} ions may have an effect on the amount of Cu_xS formed during rubber cure. As a result, the Cu/Zn ratio changes with etching time and is different for different cation containing promoters.

The sulfidation reaction is partial in the presence of stearate anion and for this reason a ZnO layer is observed in the first layer. Owing to the weak nature of this boundary layer, the adhesion is poor with stearate ions [8, 32]. This is mainly due to the fact that the bond between cobalt and stearate is weaker than that between cobalt and boroacylate, which leads to the rapid dissociation of the molecule. Because of the accelerator activating effect of the stearate ion, the sulfur and promoter are possibly used more efficiently for modification of the rubber than for the interfacial film on brass, resulting in incomplete sulfidation of the ZnO layer [8].

4. Conclusions

XPS and AES studies of the influence of cations and anions of the organometallic adhesion promoters – cobalt boroacylate, nickel boroacylate and cobalt stearate – on the interface between steel cord and natural rubber skim compounds have been reported at three etching times.

1. The atomic concentration of sulfur and carbon decreases with etching times. The oxygen concentration, however, increases marginally in the initial state before a final decrease at 15 min etching. The copper and zinc concentrations increase significantly at higher etching times. Cobalt/nickel is only found at 15 min etching.

2. Among the various organometallic adhesion promoters, the atomic concentration of copper, zinc and sulfur are highest for the system containing cobalt boroacylate.

3. The cord–rubber interface generated in the presence of cobalt boroacylate consists mainly of Cu_xS and ZnS up to 7 min etching. 15 min etching reveals the presence of Cu/CuO, ZnO/ZnS and cobalt ions. In the case of nickel boroacylate and cobalt stearate, ZnO/ZnS layer is found earlier.

References

1. E. J. WEAVER, *Rubber Plastics News* July (1978) 22.
2. W. J. VAN OOIJ, *Rubber Chem. Technol.* **51** (1978) 52.
3. L.R. BARKER, *NR-Technol.* **12** (1981) 77.
4. W.J. VAN OOIJ and M.E.F. BIEMOND, *Rubber Chem. Technol.* **57** (1984) 686.
5. P.E.R. TATE, *Rubber World* **192** (1985) 37.
6. G.R. HAMED and J. HUANG, *Rubber Chem. Technol.* **64** (1991) 857.
7. R.F. SEIBERT, in "144th meeting of the ACS (Rubber Division)", Orlando 25–29 October 1993.
8. A.K. CHANDRA, A. BISWAS, R. MUKHOPADHYAY and A.K. BHOWMICK, *J. Adhes.* **40** (1994) 177.
9. A.K. CHANDRA, A. BISWAS, R. MUKHOPADHYAY, B.R. GUPTA and A.K. BHOWMICK, *Plast. Rubb. Comp. Proc. Applic.* **22** (1994) 249.
10. W.J. VAN OOIJ, W.F. WEENING and P.F. MURRAY, *Rubber Chem. Technol.* **54** (1981) 227.
11. M. HASAN, A.K. CHANDRA, R. MUKHOPADHYAY and A.K. BHOWMICK, *Rubber World* **207** (1992) 25.
12. A. PETERSON and M.I. DIETRICK, *ibid.* **190** (1984) 24.
13. Y. ISHIKAWA, *Rubber Chem. Technol.* **57** (1984) 855.
14. A. K. CHANDRA, R. MUKHOPADHYAY and A.K. BHOWMICK, *J. Adhes. Sci. Technol.*, submitted.
15. N .L. HEWITT, *Rubber World* **205** (1991) 30.
16. P. P. LANGEVIN, R.J. PAYNE and C.S. SHEPHARD, *Rubber Chem. Technol.* **47** (1974) 171.
17. Y. ISHIKAWA and S. KAWAKAMI, *ibid.* **59** (1986) 1.
18. W.J. VAN OOIJ, *ibid.* **57** (1984) 421.
19. W.J. VAN OOIJ, J. GIRIDHAR and J.H. AHN, *Kautsch. Gummi. Kunstst.* **44** (1991) 348.
20. N. SEITZ and R. SCHMID, *ibid.* **38** (1985) 1100.
21. *Idem, ibid.* **40** (1987) 20.
22. W. COPPENS, D. CHAMBAERE and H. LIEVENS, in "International Rubber Conference", Harrogate, UK (1987).
23. W. J. VAN OOIJ, *Rubber Chem. Technol.* **52** (1979) 605.
24. A.R. MADURA, *ibid.***64** (1991) 241.
25. J. KONAR, A.K. SEN and A.K. BHOWMICK, *J. Appl. Polym. Sci.* **48** (1993) 1579.
26. J. KONAR and A. K. BHOWMICK, *J. Adhes. Sci. Technol.*, in press.
27. A. SARKAR, M.L. MUKHERJEE and A. K. BHOWMICK, *J. Mater. Sci. Lett.* **11** (1992) 924.
28. G.R. HAMED and T. DONATELLI, *Rubber Chem. Technol.* **56** (1983) 450.
29. D. BRIGGS and M.P. SEAH (eds), "Practical Surface Analysis by Auger and X-ray Photoelectron Spectroscopy" (Wiley, New York, 1984).
30. J.H. SCOFIELD, *J. Electron Spectros. Rel. Phenom.* **8** (1976) 129.
31. T.B. GHOSH and M. SREEMANY, *Appl. Surf. Sci.* **64** (1993) 59.
32. A.E. HICKS and F. LYON, in "ACS, Rubber Division, Meeting" Montreal, 2–5 May 1967, Abstract in *Rubber Chem. Technol.* **40** (1967) 1607.

Received 11 January
and accepted 7 November 1995